Design methodology and input parameters applicable to foundation design for large complex towers

Y.Y. Tay[1], BEng (Hons), PhD, CEng, FICE, FIEAust, CPEng; A. K. C. Smith[2], MA, PhD, MBA, CEng, FICE, CGeol, FGS; and C. Haberfield[3] BSc, BE (Hons), PhD, FIEAust, CPEng, RPEQ

[1, 3] Golder Associates Member of WSP, Building 7, Botanicca Corporate Park, 570-588 Swan Street, Richmond, Victoria 3121, Australia; email: ytay@golder.com.au, chaberfield@golder.com.au
[2]Coffey Geotechnics Ltd., Gardner House, Hornbeam Park Avenue, Harrogate, UK, HG5 8NA, email andrew.smith@coffey.com

ABSTRACT

As buildings are progressively getting taller, traditional methods of design that generally relied on considerations of the vertical load-carrying capacity of the foundation system, assessed by empirical methods and a lumped factor of safety, have been largely replaced by serviceability-based methods of design which typically result in an optimised foundation design. Serviceability-based designs typically rely on powerful commercial software packages to enable advanced numerical analysis of foundation systems. This paper briefly discusses case studies of foundation design processes including soil-structure interaction analyses adopted for the serviceability design of tall towers. In order to obtain accurate building movement prediction from complex computer analysis, it is imperative that materials and ground stiffness properties be accurately characterised and measured. This paper presents ground stiffness properties measured from various types of tests at different strain levels (i.e., geophysical testing, pile load tests, pressuremeter and laboratory tests) that have been adopted as input parameters in the numerical analyses. The higher allowable shaft friction values from serviceability analysis compared to those from traditional methods, are further justified on the basis of bi-directional static pile testing.

Keywords: serviceability-based design, ground stiffness, mobilised pile skin friction

1 INTRODUCTION

Serviceability-based methods of design are based on the performance and movements of building foundations rather than strength that renders the building unusable. Therefore, it is imperative that ground stiffness properties are accurately measured and appropriately adopted for foundation design. This paper presents the tests carried out in-situ and in laboratories for ground stiffness measurements of weak carbonated rock in Dubai, such as unconfined compressive strength tests with stiffness measurements, pressuremeter, geophysical and bi-directional static pile load tests. It attempts to address the strain levels at which the different tests were undertaken, amongst other variables, and therefore producing different measured stiffness range. These test strain levels were also compared to levels determined from numerical analysis of pile group foundations of tall towers when axially loaded.

2 SUBSURFACE CONDITIONS

Bedrock across the emirates of Dubai for engineering purposes is the Barzaman Formation Miocene Age rocks overlain by the more recent Quaternary Age Ghayathi Formations. The ground conditions discussed herein underlie four plots at a master development in Dubai, typically comprising superficial deposits, overlying weak calcarenite/ sandstone (Ghayathi Fm), followed by calcisiltite/ siltstone and conglomerate (Barzaman Fm). Only rock properties are discussed in this paper.

The carbonated rocks are typically weak with unconfined compressive strength (q_c) between 1.5 MPa and 4 MPa as shown in Figure 1. There is little increase in strength with depth, and no discernable difference in strength between calcarenite and calcisiltite layers (interface at around RL -25 m Dubai Municipality Datum, DMD). This was likely the result of unconfined compressive strength (UCS) tests performed without confinement and the swelling tendency of calcisiltite/ siltstone when extruded from ground at depth.

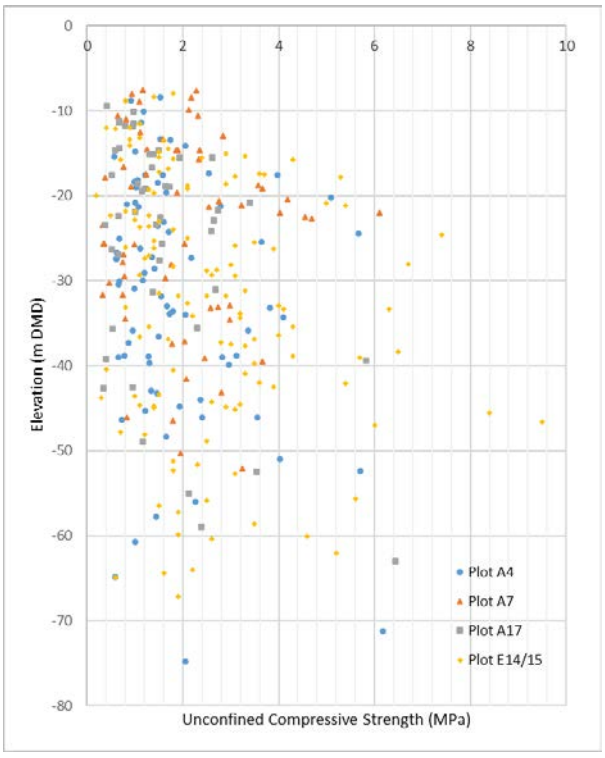

Figure 1. q_c vs depth at Plot A4, A7, A17, E14/15

3 LABORATORY AND IN-SITU TESTING

3.1 Ground stiffness measurements

In the laboratory, E_{LAB} was determined from the displacement of rock samples in UCS tests. Similar to the

q_c profile with depth, E_{LAB} values of the four plots tend not to increase significantly with depth (Figure 2).

In-situ Young's modulus (E_{PMT-H}) was measured by pressuremeter tests with unload reload cycles. The subscript "H" used here refers to measurements taken in the horizontal direction. Unload-reload $E_{PMT-H-ur}$ values from pressuremeter tests were about 4 times higher than the initial $E_{PMT-H-ini}$ (Figure 2), the main reason being that the latter was an elasto-plastic measurement where part of the expansion was irrecoverable.

Intuitively, E_{PMT-H} from pressuremeter tests which test a larger rock mass compared to intact rock samples tested in laboratory, should be smaller than E_{LAB} because of the scaling effect and the fact that the bigger rock mass is likely to consist of more imperfections, noting rock mass in Dubai do not have much fractures. However, Figure 2 shows initial $E_{PMT-H-ini}$ to be around 2.5 times higher than E_{LAB} and unload-reload $E_{PMT-H-ur}$ to be around 9 times higher than E_{LAB}. In addition, E_{PMT-H} increases with depth and the difference between E_{LAB} and E_{PMT-H} is more pronounced at depth. It is likely that E_{LAB} measurements were underestimated as a result of the lack of confinement in UCS testing and that the calcisiltite samples extruded from deeper depths were disturbed as they swelled. Other explanations of the difference between E_{LAB} and E_{PMT-H}, aside from the above and scaling effects are likely anisotropy of rock and test strain levels discussed in the following sections.

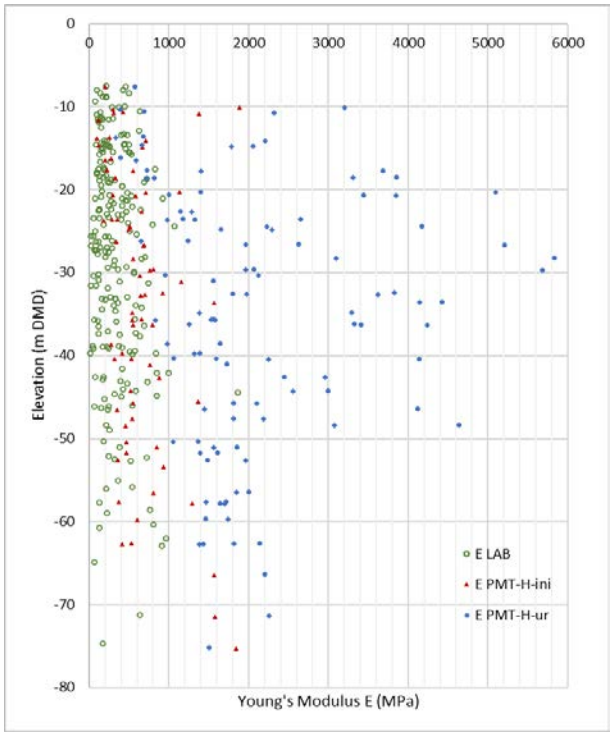

Figure 2. E_{LAB} and E_{PMT} vs depth

3.2 Correction for anisotropy

The rock mass in pressuremeter tests is loaded in the horizontal plane, and the tests give horizontal shear stiffness (G_{HH}). Whilst this may be directly applicable to the analysis of radial compression or pile lateral movement assessment, it may not be applicable for axially loaded piles where the piles and rock are deformed in the vertical plane. In the absence of direct measurements of G_{HH} and vertical shear stiffness (G_{VH}) measured from geophysical testing for anisotropy assessment, G_{HH} from pressuremeter presented in the following sections have been corrected to G_{VH} assuming anisotropy is due to the differences in normal stress acting in different directions. Therefore, stiffness in any direction is a function of K_0 as shown by the following equations from first principles:

$$G_{HH} = E_H / [2(1+ \nu_{HH})] \quad (1)$$

For undrained expansion,

$$\nu_{HH} = 1 - K_0 / 2 \quad (2)$$

$$\text{where } K_0 = E_H / E_V \quad (3)$$

E_{PMT-V} is conservatively assumed to be E_{PMT-H} / 2 in this paper, as K_0 measured from pressuremeter tests was greater than 1.5. Correction of anisotropy of rock may partly explain higher E_{PMT-H} compared to E_{LAB}.

3.3 Stiffness and strain relationship

Cavity strain measured from the expansion of borehole in pressuremeter tests was converted to shear strain. Shear strain is the constant area ratio as shown in Figure 3, therefore shear strain of the pressuremeter tests is determined from (4) below:

$$\text{Shear strain} = 1 - [\ 1/ (1+\varepsilon_c)^2\ ], \quad (4)$$

where ε_c is the cavity strain.

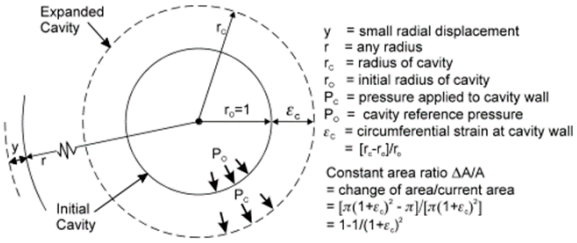

Figure 3. Pressure and straining around an expanding cavity

Figure 4 shows initial and unload-reload E_{PMT-V}, corrected for anisotropy, versus shear strain. The figure also shows combined in-situ and laboratory E measurements (i.e. E_{PMT-V}, E_{DYN} from geophysical downhole and crosshole testing and E_{LAB}) of the four plots versus their respective shear strain levels. As E values are generally consistent at strain levels less than 0.001%, maximum and minimum E_{DYN} measured was plotted at 0.001% strain in Figure 4. The shear strain of E_{LAB} has been assumed to be the strain at 50% peak stress.

From Figure 4, E values increase with decreasing shear strain which partly explains higher $E_{PMT-V-ur}$ than $E_{PMT-V-ini}$ and E_{LAB}.

4 BI-DIRECTIONAL PILE LOAD TESTS

Large scale bidirectional static load tests to failure, using Osterberg cell (O-cell), were carried out at the four plots for the assessment of pile-settlement behaviour and pile ultimate skin friction. Osterberg cell tests are increasing in popularity in Dubai. They eliminate many of the safety risks of static load tests using kentledge or tension piles. They also have the significant advantage of enabling test piles to be short enough such that full mobilisation of skin friction between the piles and ground (i.e. failure) can be achieved. The full range of the anticipated pile depths can

be tested by the simple expedient of having O-cells at different depths.

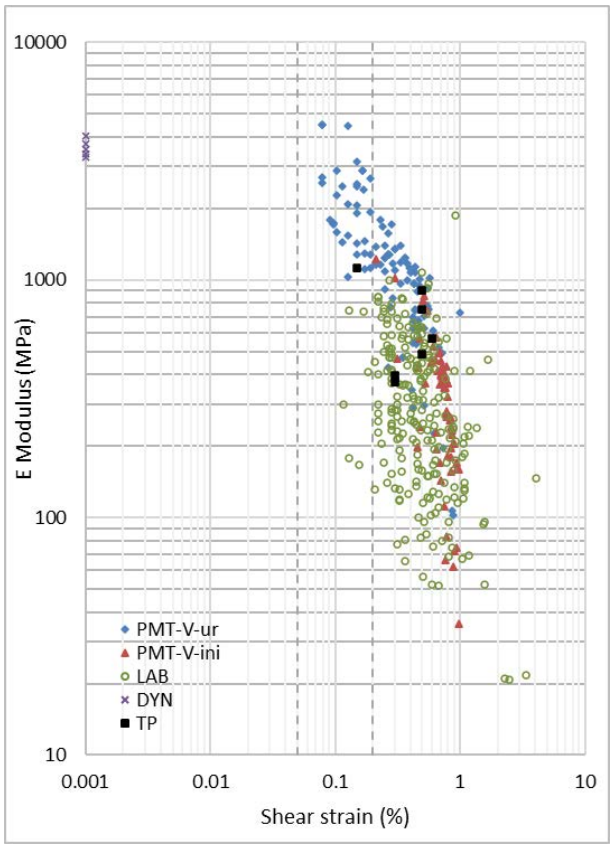

Figure 4. E Modulus versus shear strain

Each test pile carried out comprised an upper and lower segment. The segments were generally 5 to 10 m long. The test pile segments were embedded within selected depths of the rock based on strata and rock strength profiles, covering the anticipated pile depths between RL -10 m and -30 m DMD.

The test pile diameters were 1.2m at Plots A7 and A17; and 1.5m at Plots A4 and E14/15 and maximum test loads applied were 48.0MN, 53.5MN, 81.6MN and 81MN respectively. For each test pile, a number of O-cells were located at a single level separating the upper and lower test segments. The maximum test load was dependent on the number of O-cells that could be arranged across the pile section at a single level, and maximum jacking load of each O-cell that was used for testing.

A diagram showing the test pile arrangement and instrumentation is presented in Figure 5, noting that a "soft toe" had been included in majority of the test piles such that end bearing is not engaged during the testing (Figure 6).

4.1 Back analysed ground stiffness

A total of 7 no. pile tests were carried out at the four plots. Movements of the upper and lower segments of each test pile were measured as the segments were jacked apart by the O-cell. These movements were converted into an equivalent top-loaded pile-settlement curve for each test. Stiffness E_{TP} from the pile tests were back-analysed by numerical modelling a single isolated pile using Plaxis 2D (axis-symmetry model) and matching the pile-settlement in the model to that measured. E_{TP} and average shear strain along the pile, obtained from the model at pile head settlement of 1% pile diameter are included in Figure 4. The E_{TP} values fit within the range of the values determined from other tests carried out.

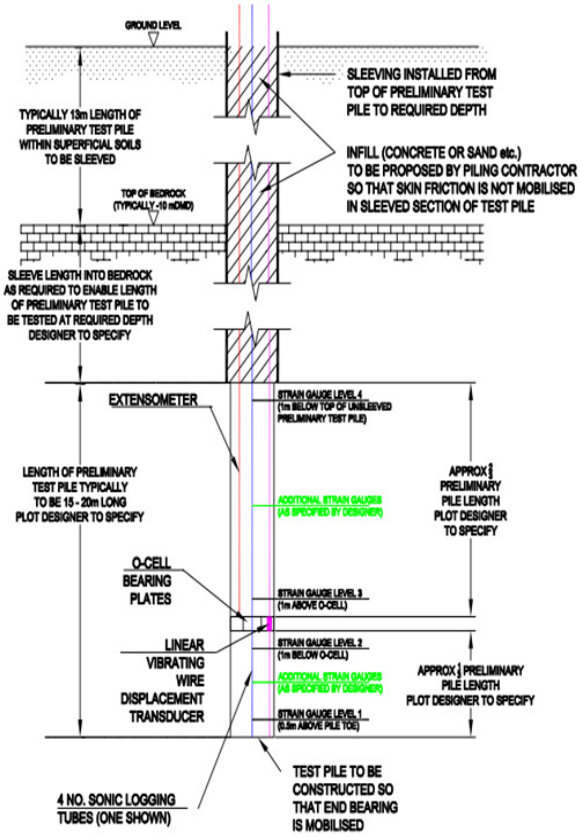

Figure 5. Diagram showing the pile arrangement

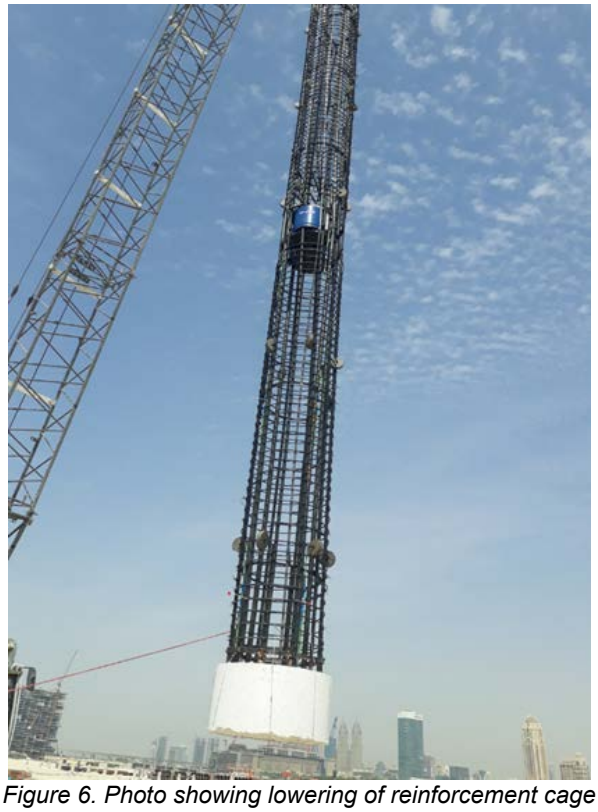

Figure 6. Photo showing lowering of reinforcement cage with 0.5m thick polystyrene 'soft toe' attached to the base

4.2 Measured pile skin friction

Average mobilised skin friction values along the upper and lower test segments of each test are shown in Figure 7. Test piles at Plots A17 and E14/15 had longer upper test segments (10m) than the lower segments (5m), the average measured values were lower for the upper segments as they were not fully mobilised. The maximum measured skin friction (near full mobilisation) at each site ranged between 1250 and 1700 kPa.

Expressions for ultimate skin friction as a function of q_c have been derived by several authors, some of which are shown in Table 1. These can typically be normalised, as shown in (5):

Ultimate skin friction = $x\sqrt{(q_c)^{0.5}}$ (5)
Where x = 0.25 to 0.4
q_c = unconfined compressive strength

Table 1. Correlations of ultimate skin friction and qc

Correlations	Reference
$0{\cdot}375\ (q_c)^{0{\cdot}515}$	Rosenberg and Journeaux (1976)
$0{\cdot}22\ (q_c)^{0{\cdot}6}$	Meigh and Wolski (1979)
$\alpha\beta\ (q_c)$	Williams and Pells (1981)
$(0{\cdot}20 \text{ to } 0{\cdot}30)\ (q_c)^{0{\cdot}5}$	Horvath et al. (1983)
$0{\cdot}45\ (q_c)^{0{\cdot}5}$	Rowe and Armitage (1987)
$0{\cdot}15\ (q_c)$	Carter and Kulhawy (1987)
$(0{\cdot}15 \text{ to } 0{\cdot}2) \times (q_c)^{0{\cdot}5}$	Reese and O'Neil (1988)
$(0{\cdot}40 \text{ to } 0.8) \times (q_c)^{0{\cdot}5}$	Zhang and Einstein (1998)

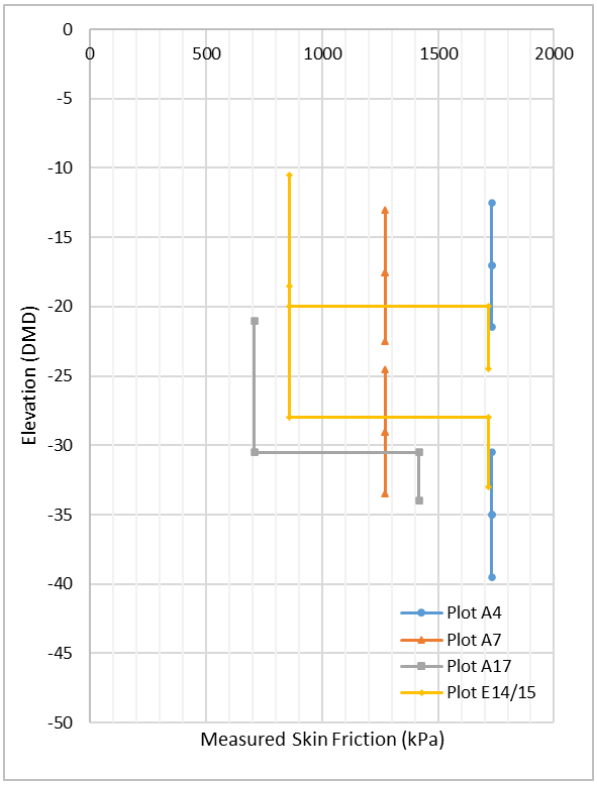

Figure 7. Average measured skin friction along test segments

Considering a mean q_c of 1.83MPa from Figure 1, ultimate unit skin friction determined from (5) would range between 450 and 730 kPa with x = 0.25 and 0.4, respectively. These values are considerably less than the measured test values, which would mean that (5) yields conservative ultimate skin friction and/or q_c values measured from UCS tests were underestimated.

5 DESIGN METHODOLOGY

The design methodology adopted for the four plots follows two slightly different but related means of achieving optimised foundation solutions by justifying serviceability analysis, also associated with higher stiffness values derived in part from pile testing; and by justifying the use of higher allowable shaft friction values on the basis of pile testing to failure.

5.1 Serviceability assessment

For serviceability-based design, soil-structure interaction modelling of foundations is key. Soil-structure interaction essentially requires compatibility between a structure, its foundation and surrounding soil/ rock. This requires two key fundamentals to be achieved, which is load equilibrium amongst the structure, foundation system and soil; and compatibly amongst displacement of structure, pile head and ground at the interfaces. The approaches to undertake soil-structure interaction assessment are:

1. 3D finite element modelling which incorporates the ground, foundation and structure.
2. Split the ground, foundation and structure into two models (structural and geotechnical models) and iterate between the models until compatible displacements at the interface of the models have been achieved.
3. 3D finite element modelling which incorporates the ground and foundation system; and column/ wall loads input as point/ line loads on the foundation system.

Assessment using Approach 1 and 2, will account for structure, foundation system and ground stiffnesses. However, structure stiffness will not be accounted for in Approach 3. Furthermore, redistribution of column loads (if any) as a result of foundation displacement will not be captured. The robustness of design is often inversely proportional to the duration required to construct the model for assessment. Therefore, whilst Approach 1 provides the most robust of designs, it is often impracticable for use given that the project timeframe is usually short. It will also require both structural and geotechnical engineers working on a single model to ensure specific elements are correctly modelled. The following discusses methodology and input parameters adopted for Plot A4. A similar process was followed for all other plots.

A non-linear strain dependent stiffness curve is ideal as input for assessment by Approach 1. However due to time constraints, Approach 2 with characteristic $E_{PMT\text{-}H\text{-}ini}$ values was adopted for the pile group design, noting that the geotechnical software used did not allow for non-linear stiffness analysis. Characteristic $E_{PMT\text{-}H\text{-}ini}$ values were not corrected for rock anisotropy, and were assumed to lie between $E_{PMT\text{-}V\text{-}ini}$ and $E_{PMT\text{-}V\text{-}ur}$ as shown in Figure 8.

The strain range of axially loaded pile groups determined from numerical assessment is around 0.2%, which is at the higher end of typical strains for foundation indicated by Atkinson (2000) as shown in Figure 9.

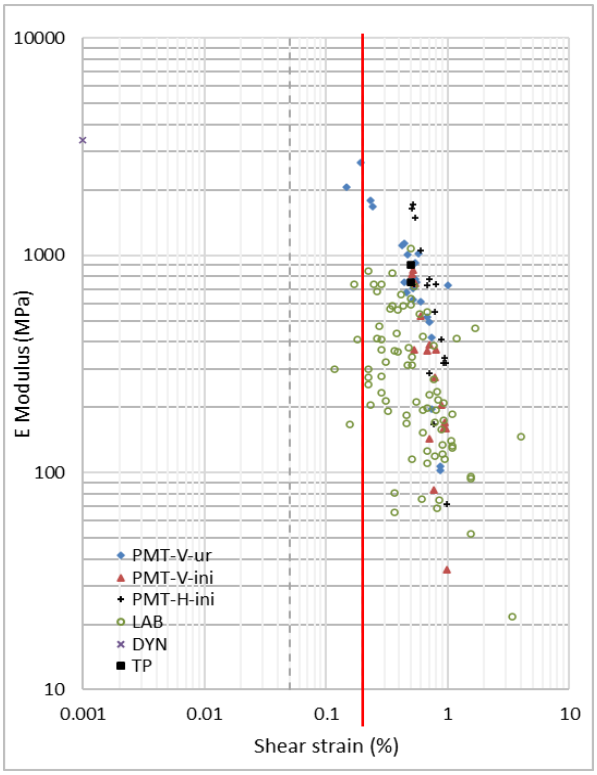

Figure 8. E Modulus versus shear strain - Plot A4

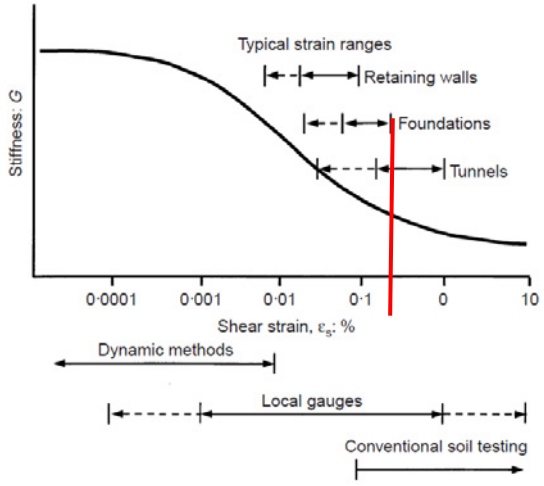

Figure 9. Typical strain ranges for geotechnical structures (Atkinson, 2000)

Considering stiffness E associated with the strain range of pile group foundations (around 0.2%) and the back-analysed E_{TP} from pile tests (see Figure 8), the use of $E_{PMT\text{-}H\text{-}ini,}$ (uncorrected for anisotropy) in the design is justified.

5.2 Pile skin friction

Allowable skin friction (fs) values for Plot A4 were determined based on the following methods for comparison purpose:

1. Traditional method of applying a lumped factor of 2.5 to ultimate f_s determined from (5) with q_c from site investigation.
2. Back-analysed from serviceability analysis adopting $E_{PMT\text{-}H\text{-}ini}$ and a limiting total building settlement of 50mm.
3. Applying a factor of safety of 2.5 to measured skin friction from pile testing to near failure. The factor of safety includes the additional design criterion that attempts to avoid the full mobilisation of shaft friction along the piles to reduce the risk that cyclic loading will lead to degradation of shaft capacity for tall tower foundations (Poulos, 2017), especially those embedded in weak carbonated rock.

Figure 10 shows allowable pile skin friction determined from the three methods, and values from Method 1 were conservative. Serviceability analysis (Method 2) offers a more economical design, where the lengths of the piles were shorter with higher allowable skin friction compared to Method 1. Should higher allowable building settlement (i.e. > 50 mm) be considered, the pile design may be further revised. However, allowable friction values from Method 2 should not exceed values from Method 3, in which potential pile skin friction degradation is considered. Adopting factored friction values from pile tests (Method 3) alone without settlement checks, would result in movements outside the limiting tolerance as the piles were tested to failure.

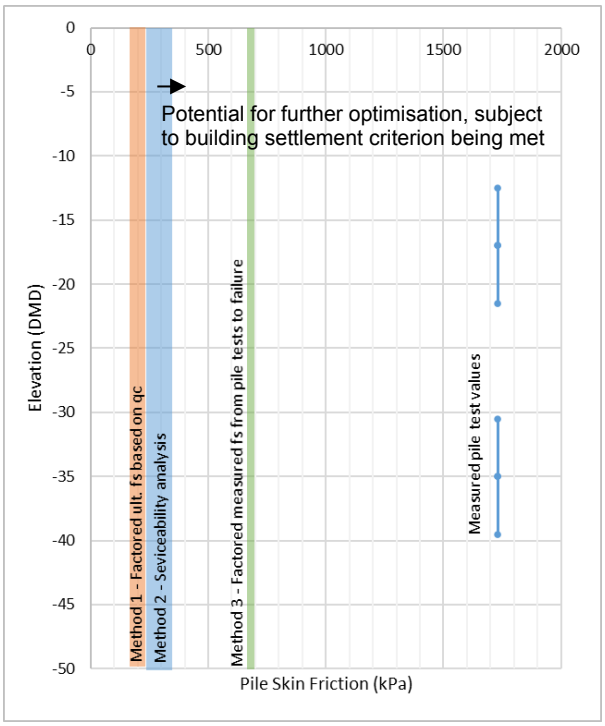

Figure 10. Pile skin friction – Plot A4

6 CONCLUSION

This paper discusses the design methodology that follows two slightly different but related means of achieving optimised foundation solutions by justifying serviceability analysis with the use of high stiffness values and by justifying the use of higher allowable shaft friction values on the basis of pile testing.

A brief overview of soil-structure interaction assessment methods is presented, along with ground stiffness measurements from various testing at different strain levels for serviceability analysis. Case studies show that allowable skin friction values determined from serviceability analysis were higher than those from empirical formula with a lumped factor of safety. The use of allowable skin friction from serviceability analyses were further justified by measured skin friction values, from

large scale bi-directional static pile tests to failure, which were reduced to avoid the full mobilisation of shaft friction along the piles. This is partly to reduce the risk associated with cyclic loading that will lead to degradation of shaft capacity for tall tower foundations embedded in carbonated weak rock.

7 ACKNOWLEDGEMENTS

The work presented in this paper was carried out by the authors on projects in Dubai with the support of their colleagues at Tetra Tech Coffey. They are thankful to Antone Dabeet and Nabeel Bux who provided expertise that greatly assisted the projects.

REFERENCES

Atkinson JH (2000), “Non-linear soil stiffness in routine design.” Géotechnique, 50(5), 487–508.

Carter JP and Kulhawy FH (1987), “Analysis and Design of Foundations Socketed into Rock”. Geotechnical Engineering Group, Cornell University, Ithaca, NY, USA, Res. Rep. 1493-4.

Horvath RG, Kenney TC and Kozicki P (1983), “Methods of improving the performance of drilled piers in weak rock”. Canadian Geotechnical Journal 20(4), 758-772.

Meigh AC and Wolski W (1979), “Design parameters for weak rock”. Proceedings of 7th European Conference on Soil Mechanics and Foundation Engineering. British Geotechnical Society, London, UK, vol. 5, pp. 59–79.

Poulos HG (2017), “Tall Building Foundation Design.” CRC Press, Boca Raton, USA.

Reese LC and O’Neill MW (1988), “Drilled Shafts: Construction Procedures and Design Methods”. US Department of Transportation, Dallas, TX, USA, FHWA-HI-88-042.

Rosenberg P and Journeaux NL (1976), “Friction and end bearing tests on bedrock for high capacity socket design”. Canadian Geotechnical Journal 13(3), 324–333.

Rowe RK and Armitage HH (1987), “Theoretical solution for axial deformation of drilled shaft”. Canadian Geotechnical Journal 24(1), 114–125.

Williams AF and Pells PJN (1981), “Side resistance rock sockets in sandstone, mudstone, and shale”. Canadian Geotechnical Journal 18(4), 502–513.

Zhang L and Einstein HH (1998), “End bearing capacity of drilled shafts in rock”. Journal of Geotechnical and Geoenvironmental Engineering 124(7), 574–584.